Journal of Computational and Applied Mathematics 424 (2023) 115014

Contents lists available at ScienceDirect

Journal of Computational and Applied Mathematics

journal homepage: www.elsevier.com/locate/cam

A generalized midpoint-based boundary value method for unstable partial differential equations

P.A. Zegeling [a,*], M.W.F. van Spengler [b]

[a] Utrecht University, Budapestlaan 6, 3584 CD Utrecht, The Netherlands
[b] University of Amsterdam, Science Park 904, 1098 XH Amsterdam, The Netherlands

ARTICLE INFO

Article history:
Received 6 January 2022
Received in revised form 28 September 2022

Keywords:
Boundary value method
Stability region
Numerical stability
Space-fractional heat equation
Backward heat equation

ABSTRACT

We present a class of Boundary Value Methods (BVMs) that can be applied to semi-stable and unstable Partial Differential Equation (PDE) models. Step-by-step (initial value) methods, such as Runge–Kutta and linear multistep methods have numerical stability regions which do not intersect with certain regions of the complex plane that are significant to the time-integration of unstable PDEs. BVMs, which need extra numerical conditions at the final time, are global methods and are, in some sense, free of such barriers. We discuss BVMs based on generalized midpoint methods, combined with appropriate numerical initial and final conditions. The stability regions of these methods intersect with a significant part of the complex plane. In several numerical experiments we will illustrate the usefulness of such methods when applied to PDE models, such as a dispersive wave equation, a space-fractional PDE and the backward heat equation.

1. Introduction

In this paper we investigate Partial Differential Equations (PDEs) of the form:

$$\begin{cases} \frac{\partial u}{\partial t}(x,t) = \mathcal{L}u(x,t), \quad (x,t) \in \mathbb{R} \times (0,T], \\ u(x,0) = u_0(x), \end{cases} \tag{1}$$

with spatial differential operator $\mathcal{L}$, plus the corresponding boundary conditions and initial condition $u_0(x)$. Of special interest in this paper are the cases where the operator $\mathcal{L}$ describes processes with unstable or both stable and unstable regions in its domain during the time evolution $t > 0$. To be more precise, we assume in this paper that the spectrum of $\mathcal{L}$ may contain regions within the entire complex plane. When $\mathcal{L}$ has both regions in the left half (stable region) and the right half (unstable region) of the complex plane, then we call PDE (1) a semi-stable model. Examples of such models in practical applications are given by combustion processes (flame propagation) [1,2], dispersive wave equations [3–5], backward-heat equations [6–9] and may appear in fractional-order differential equations [10–13].

Customarily, only differential equations where the entire spectrum of $\mathcal{L}$ has negative real part are considered [14–16]. This is due to the fact that the instability of unstable differential equations often implies instability of numerical integration methods. For example, initial value methods (IVMs), also known as linear multistep methods, generally suffer from instabilities when applied to an unstable system. This convention of ignoring unstable models has also made its way into much of the literature on Boundary Value Methods (BVMs). However, as will be shown in this paper, such a

* Corresponding author.
E-mail address: P.A.Zegeling@uu.nl (P.A. Zegeling).

https://doi.org/10.1016/j.cam.2022.115014

severe restriction is unnecessary for these methods. Note that our goal is to describe and explain the numerical stability properties of the proposed BVMs. We do not aim, however, at comparing the accuracy between BVMs and IVMs.

In Section 2, we will shortly describe BVMs and their relation to IVMs. Moreover, we will introduce a specific class of BVMs which can be applied stably to unstable differential equations, namely the class of generalized midpoint-based BVMs. Then, some theory and analysis on the accuracy and stability properties of these methods is discussed in Section 3. Numerical results to support the theoretical considerations are described in Section 4. Finally, Section 5 summarizes our findings.

2. Generalized midpoint-based boundary value methods

For simplicity, we will first consider initial-value problems of the form

$$\begin{cases} u'(t) = f(u(t), t), \quad t \in [0, T], \\ u(0) = u_0. \end{cases} \tag{2}$$

Such problems can be solved approximately on some finite grid using Boundary Value Methods (BVMs), which are described extensively in [17–19] and which can be seen as a generalization of initial value methods (IVMs). In short, a BVM consists of two components. The first is a linear multistep formula (LMF) of the form

$$\sum_{j=0}^{k} \alpha_j u_{n+j} - \Delta t \sum_{j=0}^{k} \beta_j f_{n+j} = 0, \tag{3}$$

applied over some uniform finite grid $t_0, \ldots, t_N \in [0, T]$, where

$$u_n \approx u(t_n), \quad f_n \approx f(u(t_n), t_n),$$

and where Δt is the constant time-step. A well-known example of such an LMF is the explicit midpoint formula given by

$$\frac{1}{2} u_{n+1} - \frac{1}{2} u_{n-1} = \Delta t f_n. \tag{4}$$

In order to solve the resulting system of equations, k boundary conditions are required of which only one is given, namely the initial condition $u(0) = u_0$. The second component of a BVM is the choice of the $k - 1$ additional conditions which can be chosen either at the start of the domain or at the end of the domain so at $t = 0$ or $t = T$, respectively. These conditions are generally chosen to be in the form of LMF as well, so in the form of Eq. (3), and are called the additional initial and final conditions. The number of initial conditions is denoted by $k_1 \geq 1$ and the number of final conditions by $k_2 \geq 0$ with $k = k_1 + k_2$. The resulting BVM is called a (k_1, k_2)-BVM. To see that BVMs are indeed a generalization of IVMs, observe that the methods where $k_2 = 0$, so the $(k, 0)$-BVMs, are IVMs.

Note that for an IVM of order p, the order of the additional initial conditions should be at least $p - 1$ to ensure that the errors are actually behaving as expected [17]. The same condition on the order of the boundary conditions holds for BVMs, as can be seen from the proof of convergence of these methods, given in [17]. To ensure that the error consists mainly of the errors introduced by the choice of LMF, the boundary conditions will be chosen to be of the same order as the LMF.

Some well-known classes of IVMs have been generalized to BVMs. Examples are the generalized backward differentiation formulae and the generalized Adams methods, which are discussed in, for example, [17]. In this paper, a class of symmetric BVMs will be discussed which has some desirable properties for dealing with unstable problems of the form (2). A symmetric method uses an LMF with the property that

$$\alpha_i = -\alpha_{k-i}, \qquad \beta_i = \beta_{k-i}, \quad i = 0, \ldots, k. \tag{5}$$

Such methods are also described in [17], but there the discussion is restricted mostly to the case where k is odd, so for example any BVM which uses the trapezoidal LMF. Here, however, we will consider methods where k is even, so where we can write $k = 2\nu$. Examples of these methods are BVMs which apply the midpoint LMF (4) or the Simpson LMF. The class of methods that we will discuss can be seen as a generalization of the midpoint BVM, as described in [20].

Note that the midpoint LMF (4) is the formula that one obtains by setting

$$\begin{cases} \beta_i = 0, \quad i \neq \nu = \frac{k}{2}, \\ \beta_\nu = 1, \end{cases} \tag{6}$$

and by choosing the α_i such that the LMF is of the highest order of accuracy. Thus, an obvious generalization of this LMF is to perform this process for arbitrary $k = 2\nu$. As shown in, for example, [17], the maximal order of accuracy that is

Table 1
Coefficients of the first four generalized midpoint LMF.

k	ν	$\alpha_{\nu-4}$	$\alpha_{\nu-3}$	$\alpha_{\nu-2}$	$\alpha_{\nu-1}$	α_{ν}	$\alpha_{\nu+1}$	$\alpha_{\nu+2}$	$\alpha_{\nu+3}$	$\alpha_{\nu+4}$
2	1				$-\frac{1}{2}$	0	$\frac{1}{2}$			
4	2			$\frac{1}{12}$	$-\frac{8}{12}$	0	$\frac{8}{12}$	$-\frac{1}{12}$		
6	3		$-\frac{1}{60}$	$\frac{9}{60}$	$-\frac{45}{60}$	0	$\frac{45}{60}$	$-\frac{9}{60}$	$\frac{1}{60}$	
8	4	$\frac{3}{840}$	$-\frac{32}{840}$	$\frac{168}{840}$	$-\frac{672}{840}$	0	$\frac{672}{840}$	$-\frac{168}{840}$	$\frac{32}{840}$	$-\frac{3}{840}$

attainable in this fashion is k. This LMF is found by solving the linear system

$$\begin{pmatrix} 1 & 1 & \cdots & 1 \\ 0 & 1 & \cdots & k \\ 0 & 1^2 & \cdots & k^2 \\ \vdots & \vdots & & \vdots \\ 0 & 1^k & \cdots & k^k \end{pmatrix} \begin{pmatrix} \alpha_0 \\ \alpha_1 \\ \vdots \\ \alpha_k \end{pmatrix} = \begin{pmatrix} 0 \\ 1 \\ 2\nu \\ \vdots \\ k\nu^{k-1} \end{pmatrix}. \tag{7}$$

One can show that the resulting coefficients in fact satisfy the symmetry relations (5). The proof of this statement is a simplification of the proof for the generalized Simpson LMF in [17]. The α-coefficients of these LMF for $\nu = 1, 2, 3, 4$ are shown in Table 1. Coefficients of some higher order methods are shown in Appendix B.

We define the νth generalized midpoint-based BVM as the BVM which applies the νth LMF as described above with $\nu - 1$ additional initial conditions given by

$$\sum_{j=0}^{k} \tilde{\alpha}_{j,r} u_{k-j} = \Delta t f_{\nu-r}, \quad r = 1, \ldots, \nu - 1, \tag{8}$$

and ν additional final conditions given by

$$\sum_{j=0}^{k} \alpha_{j,r} u_{N-k+j} = \Delta t f_{N+r-\nu}, \quad r = 1, \ldots, \nu, \tag{9}$$

where the $\alpha_{j,r}$ satisfy the systems

$$\begin{pmatrix} 1 & 1 & \cdots & 1 \\ 0 & 1 & \cdots & k \\ 0 & 1^2 & \cdots & k^2 \\ \vdots & \vdots & & \vdots \\ 0 & 1^k & \cdots & k^k \end{pmatrix} \begin{pmatrix} \alpha_{0,r} \\ \alpha_{1,r} \\ \vdots \\ \alpha_{k,r} \end{pmatrix} = \begin{pmatrix} 0 \\ 1 \\ 2(\nu + r) \\ \vdots \\ k(\nu + r)^{k-1} \end{pmatrix}, \quad r = 1, \ldots, \nu, \tag{10}$$

and where we let $\tilde{\alpha}_{j,r} = -\alpha_{j,r}$ for all j and r. As shown in Appendix A, the resulting boundary conditions are of the order k as well, which is a preferable choice as will become apparent in the next section. Note that Eq. (10) is easily derived from the order conditions for a general pth order LMF

$$\sum_{j=0}^{k} (j^s \alpha_j - s j^{s-1} \beta_j) = 0, \quad s = 0, 1, \ldots, p. \tag{11}$$

Furthermore, the resulting methods can be shown to be unconditionally stable when applied to problems of the form (2), as will be shown in the next section. The coefficients of the additional boundary conditions up to $\nu = 4$ are shown in Appendix C.

3. Theory and analysis

In the theoretical discussion within this section, we shall restrict ourselves to the case of the linear test equation defined by

$$u' = \lambda u, \quad \lambda \in \mathbb{C}, \tag{12}$$

as these results can easily be extended to the general case. Note that we do not exclude unstable equations where λ has positive real part. For simplicity, we introduce the variable $q = \lambda \Delta t$.

In the discussion that follows, the characteristic polynomial of an LMF will be used extensively. This polynomial is defined as

$$\pi(z,q) = \rho(z) - q\sigma(z), \tag{13}$$

where

$$\rho(z) = \sum_{j=0}^{k} \alpha_j z^j, \qquad \sigma(z) = \sum_{j=0}^{k} \beta_j z^j. \tag{14}$$

Furthermore, some specific types of polynomials will be of importance, namely $N_{k_1k_2}$-polynomials and $S_{k_1k_2}$-polynomials. The prior are defined as polynomials of which k_1 roots lie on the closed unit disk and k_2 roots lie outside of the closed unit disk in the complex plane, whereas the latter are defined as those polynomials for which k_1 roots lie on the open unit disk and k_2 roots lie outside the closed unit disk.

3.1. Stability regions and properties of BVMs

Brugnano and Trigiante provide a generalization of the Dahlquist equivalence theorem in [17,21], which states that a (k_1, k_2)-BVM is convergent if it is consistent and if the polynomial $\rho(z)$ of the corresponding LMF, as defined in Eq. (14), is of type $N_{k_1k_2}$. Alongside this, we require stability of a method for some fixed Δt in order for it to be applicable. For IVMs, one can show that a method is absolutely stable for some choice of Δt if the resulting characteristic polynomial $\pi(z,q)$ is a Schur polynomial, so a polynomial of type S_{k0}. For a proof of this result, see for example [14,22]. Due to this result, the region in the complex q-plane where $\pi(z,q)$ is a Schur polynomial is often called the region of absolute stability of an LMF.

The definition of the region of absolute stability has been generalized to the case of (k_1, k_2)-BVMs in [17,21,23,24]:

Definition 3.1 (*Region of* (k_1, k_2)*-absolute Stability*)**.** The region

$$\mathcal{D}_{k_1,k_2} = \{q \in \mathbb{C} : \pi(z,q) \text{ is } S_{k_1k_2}\},$$

is called the region of (k_1, k_2)-absolute stability of an LMF.

One can show that the system of finite difference equations, that results from some choice of (k_1, k_2)-BVM and fixed Δt, is indeed stable if $\pi(z,q)$ is of type $S_{k_1k_2}$. The proof of this result is a generalization of the proof, given in [17], for the case where $k_1 = k$ and it will be shown in the upcoming paper [25]. A sketch of this proof is given in Appendix D.

Note that the regions of absolute stability for different choices of k_1 and k_2 are separated by the set in the complex q-plane for which $\pi(z,q)$ has a root of unit modulus. This curve is called the boundary locus and is commonly denoted by Γ. We can parameterize this curve as

$$\Gamma = \{q(e^{i\theta}) \in \mathbb{C} : \theta \in [0, 2\pi)\}, \tag{15}$$

where

$$q(z) = \frac{\rho(z)}{\sigma(z)}. \tag{16}$$

Some easily verifiable properties of this curve are that it always contains the origin if the corresponding LMF is consistent and that it is symmetric with respect to the real axis. In what follows, it will be shown that the regions of absolute stability of the generalized midpoint-based BVMs have a rather advantageous property.

3.2. Stability properties of generalized midpoint-based BVMs

A first observation to make is that, for a symmetric LMF, the polynomials $\rho(z)$ and $\sigma(z)$ from Eq. (14) satisfy

$$\rho(z) = -z^k \rho(z^{-1}), \qquad \sigma(z) = z^k \sigma(z^{-1}). \tag{17}$$

Using this observation, we can show that the boundary locus of any symmetric method is contained in the imaginary axis, since

$$\begin{aligned}\Re(q(e^{i\theta})) &= \frac{1}{2}\left(\frac{\rho(e^{i\theta})}{\sigma(e^{i\theta})} + \overline{\frac{\rho(e^{i\theta})}{\sigma(e^{i\theta})}}\right) = \frac{1}{2}\left(\frac{\rho(e^{i\theta})}{\sigma(e^{i\theta})} + \frac{\rho(e^{-i\theta})}{\sigma(e^{-i\theta})}\right) \\ &= \frac{e^{-ik\theta}}{2\sigma(e^{i\theta})\sigma(e^{-i\theta})}\left(\rho(e^{i\theta})\sigma(e^{i\theta}) - \rho(e^{i\theta})\sigma(e^{i\theta})\right) = 0.\end{aligned}$$

Moreover, for the LMF involved in the generalized midpoint-based BVMs, we find $\sigma(z) = z^\nu$. So, $\sigma(z)$ has no roots of unit modulus from which it follows that the boundary locus is bounded. Thus, the boundary locus of these LMF is a bounded interval of the imaginary axis which is symmetrical around the origin. Therefore, we obtain

$$\mathcal{D}_{k_1k_2} = \mathbb{C} \setminus \Gamma, \tag{18}$$

for some k_1 and k_2.

Another interesting property of the midpoint LMF is that their characteristic polynomials satisfy

$$\pi(z, q) = \rho(z) - q\sigma(z) = -z^k\big(\rho(z^{-1}) + q\sigma(z^{-1})\big) = -z^k\pi(z^{-1}, -q). \tag{19}$$

It follows from this property that, if ξ is a root of $\pi(z, q)$, then ξ^{-1} is a root of $\pi(z, -q)$, and thus that, if $\pi(z, q)$ is of type $S_{k_1k_2}$, then $\pi(z, -q)$ is of type $S_{k_2k_1}$. Combining this with Eq. (18) shows that, for the LMF of midpoint-based BVMs:

$$\mathcal{D}_{\nu\nu} = \mathbb{C} \setminus \Gamma. \tag{20}$$

As a result, the stability of the generalized midpoint-based BVMs, as defined in the previous section, does not depend on the eigenvalues of the problem. This property makes these methods especially useful when dealing with semi-stable differential equations where the eigenvalues of the corresponding differential operator can lie in both the left half and the right half of the complex plane, as will be shown in the next section.

In [17] it is shown that for k odd the left and right halves of the complex plane belong to different regions of absolute stability. Therefore, these methods cannot be properly applied when the spectrum of the relevant differential operator contains values with positive real part and values with negative real part. This is why we have restricted ourselves to the case where k is even.

3.3. Generalized midpoint-based BVM with $\nu = 2$

As an example, consider the generalized midpoint LMF for $\nu = 2$. The coefficients are given in Table 1. The corresponding characteristic polynomial reads: $\pi(z, q) = -\frac{1}{12}z^4 + \frac{8}{12}z^3 - qz^2 - \frac{8}{12}z + \frac{1}{12}$. Note that zero is the only root of the polynomial $\sigma(z)$, so the boundary locus is indeed bounded. Moreover, it follows from the previous subsection that the boundary locus is contained in the imaginary axis. Therefore, Γ is a closed interval of the imaginary axis. Lastly, if we check, for example, the case $q = 1$, one easily verifies that $\pi(z, 1)$ is of type $S_{2,2}$, from which it follows that $\mathcal{D}_{2,2} = \mathbb{C} \setminus \Gamma$. Thus, this LMF is unconditionally stable for fixed Δt, if it is applied with two initial and two final conditions.

4. Numerical results

By applying a BVM to a linear system of differential equations, a single large linear system is obtained. Contrary to systems obtained from IVMs, this system generally cannot be solved in a step-by-step fashion. Thus, when applying a BVM to solve a system of m ODEs, a linear system of $Nm \times Nm$ has to be solved. On the other hand, in case of an explicit IVM, the numerical solution only requires N matrix vector multiplications involving a km $\times$ km matrix and an implicit IVM only requires solving N linear systems involving a km $\times$ km matrix. Clearly, for relatively small k, both types of IVMs are significantly less expensive than BVMs. In the results that follow, each linear system was solved using MATLAB's *mldivide*-routine as documented in [26].

4.1. A semi-stable ODE

The first example is a semi-stable Ordinary Differential Equation (ODE) and reads:

$$\begin{cases} u'(t) = \cos(t)\, u(t), \quad t \in [0, T], \\ u(0) = 1, \end{cases} \tag{21}$$

with exact solution $u(t) = \mathrm{e}^{\sin(t)}$. Fig. 1 shows numerical results obtained by applying Explicit Euler (EE), Implicit Euler (IE) and the midpoint BVM ($\nu = 1$) in the interval $t \in [0, 20]$ for $\Delta t = 0.1$. We observe in the left frame that the absolute errors for EE and IE grow rapidly, while the BVM errors remain bounded and small. The right frame in Fig. 1 confirms the second-order behaviour of the BVM method for $\nu = 1$. Note that these EE and IE results would be characteristic for *any* explicit and implicit time-integration method. In Fig. 2 we show the large difference in accuracy between EE (left frame; indicated by FT = Forward in Time) and the midpoint BVM (right frame) for $\Delta t = 0.1$ on the extended time interval $t \in [0, 100]$.

4.2. A dispersive wave equation

The second model is a mixed higher-order ("dispersive-wave") PDE of the form:

$$\begin{cases} u_{tt}(x, t) = u_{xxx}(x, t), \quad (x, t) \in [0, 1] \times [0, T], \\ u(x, 0) = \sin(2\pi x), \quad u_t(x, 0) = 0, \\ u(0, t) = u(1, t), \ u_x(0, t) = u_x(1, t), \ u_{xx}(0, t) = u_{xx}(1, t), \end{cases} \tag{22}$$

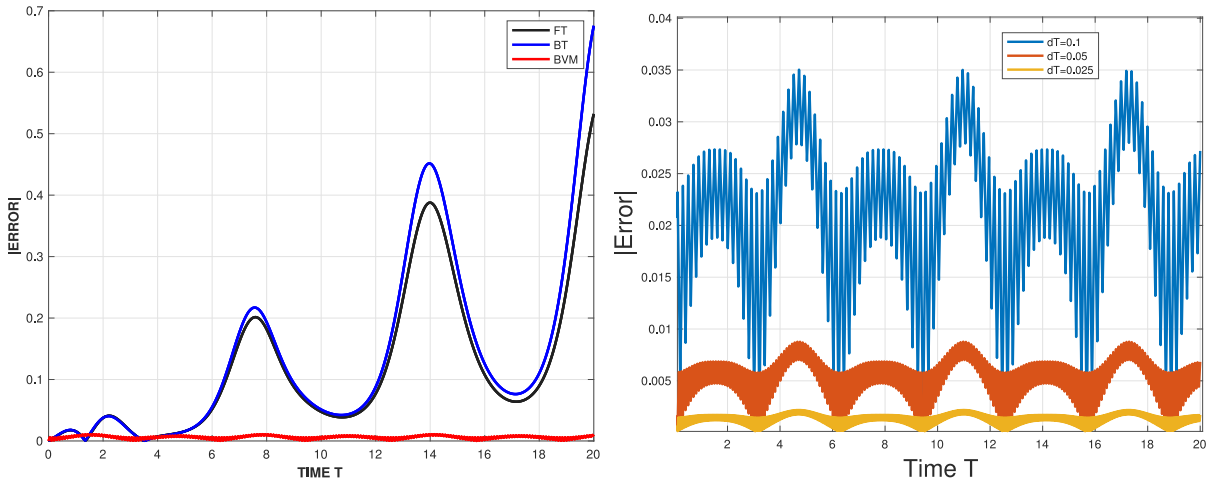

Fig. 1. In the left frame, the numerical errors for model (21) with $\Delta t = 0.1$ are displayed for Explicit Euler (black; indicated by FT = Forward in Time), Implicit Euler (blue; indicated by BT = Backward in Time) and a midpoint-BV method (red), respectively. The BVM outperforms the explicit and implicit method completely. In the right frame we recognize the second-order convergence of the midpoint-BV method ($\nu = 1$): the error goes down with a factor of four when decreasing the time step size with a factor of two.

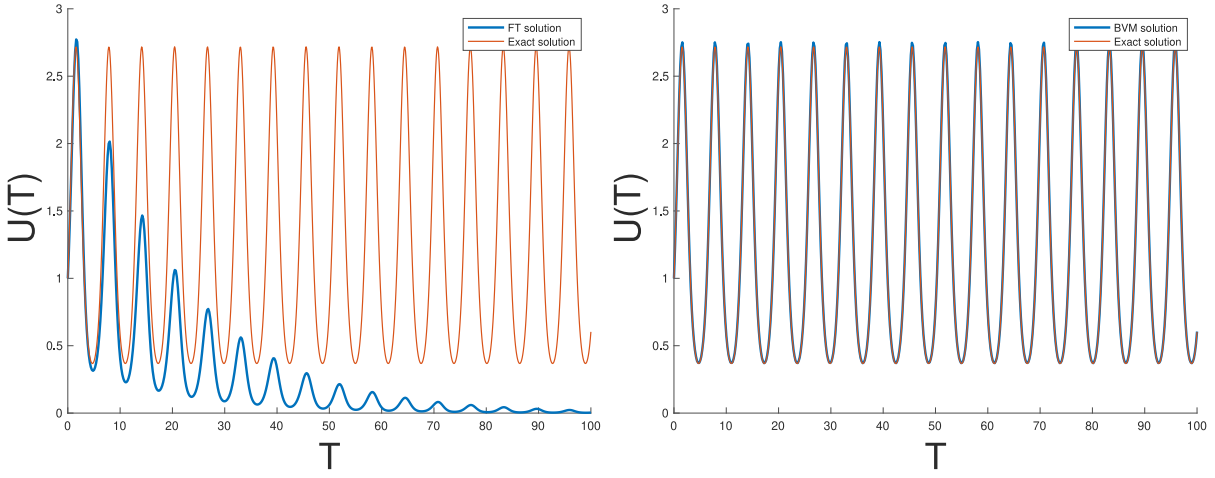

Fig. 2. In the left frame, we show the explicit Euler solution with $\Delta t = 0.1$ (blue) for model (21) in comparison with the exact solution (orange) on the time interval $t \in [0, 100]$. In the right frame the BVM ($\nu = 1$) solution with $\Delta t = 0.1$ (blue) for ODE model (21) shows an almost perfect match with the exact solution (orange).

with exact solution $u(x,t) = \frac{1}{2}[e^{2\pi \frac{3}{2} t} \sin(2\pi x - 2\pi \frac{3}{2} t) + e^{-2\pi \frac{3}{2} t} \sin(2\pi x + 2\pi \frac{3}{2} t)]$. This PDE model has applications, among others, in hydrodynamics [3,5], and potential theory [4]. It can be written as a system of first-order (in time) PDEs:

$$\begin{cases} u_t(x,t) := v(x,t), \\ v_t(x,t) = u_{xxx}(x,t) := D^3[u(x,t)]. \end{cases} \tag{23}$$

Semi-discretization of system (23), following the Method-Of-Lines, gives:

$$\begin{cases} \dot{\vec{u}}(t) = \vec{v}(t), \\ \dot{\vec{v}}(t) = \mathcal{D}_3\, \vec{u}(t). \end{cases} \Leftrightarrow \quad \dot{\vec{y}}(t) = \begin{pmatrix} \mathcal{O} & \mathcal{I} \\ \mathcal{D}_3 & \mathcal{O} \end{pmatrix} \vec{y}(t) := \mathcal{C}\, \vec{y}(t). \tag{24}$$

Here, $\mathcal{D}_3$ represents the finite-difference matrix of a second-order central approximation for the third derivative u_{xxx}:

$$u_{xxx}|_{x=x_i} \approx \frac{1}{2(\Delta x)^3}\Big(u_{i+2} - 2u_{i+1} + 2u_{i-1} - u_{i-2}\Big), \tag{25}$$

Table 2
Maximum absolute errors at $t = 0.3$ and cpu-time in seconds for BVM ($\nu = 1$), applied to model (22), Explicit Euler (EE) and Implicit Euler (IE) and decreasing values of Δt with a fixed $\Delta x = 0.0125$.

$\Delta x = 0.0125$	BVM_{er}	BVM_{ti}	FT_{er}	FT_{ti}	BT_{er}	BT_{ti}
$\Delta t = 0.01600$	11.5146	0.02	$\mathcal{O}(10^{5})$	0.0105	0.5532	0.0199
$\Delta t = 0.00400$	0.7859	0.11	$\mathcal{O}(10^{19})$	0.0092	0.1528	0.0310
$\Delta t = 0.00100$	0.0508	1.84	$\mathcal{O}(10^{71})$	0.0096	$\mathcal{O}(10^{35})$	0.1061
$\Delta t = 0.00025$	0.0056	43.71	$\mathcal{O}(10^{86})$	0.0177	$\mathcal{O}(10^{104})$	0.4053

Table 3
Maximum absolute errors at $t = 0.3$ for BVM ($\nu = 1$), applied to model (22), for different stepsizes Δt and Δx.

BV-method ($\nu = 1$)	$\Delta x = 0.2$	$\Delta x = 0.1$	$\Delta x = 0.05$	$\Delta x = 0.025$
$\Delta t = 0.0020$	0.9104	0.3628	0.2170	0.2012
$\Delta t = 0.0010$	0.8462	0.2859	0.0891	0.0561
$\Delta t = 0.0005$	0.8305	0.2648	0.0650	0.0223
$\Delta t = 0.00025$	0.8265	0.2598	0.0611	0.0160

together with periodic boundary conditions. Note that the eigenvalues of the matrix $\mathcal{D}_3$ are purely imaginary, and that, therefore, the eigenvalues of $\mathcal{C}$ lie in the complex plane under an angle of 45 and 135 degrees, as shown in the upper left frame of Fig. 3. Also in Fig. 3, numerical results at $t = 0.4$ are shown for FTCS (Explicit Euler, upper right frame) and BTCS (Implicit Euler, middle left frame), both with the spatial discretization (25). These methods diverge for decreasing Δt, due to the fact that the eigenvalues of $\mathcal{C}$ lie outside of their respective stability regions for Δt small enough. The middle right frame displays the generalized midpoint-based method ($\nu = 1$) solution as a function of Δt at $t = 0.4$. Lastly, as comparison with another higher order symmetric BVM but with k odd, the two lower frames show the solutions when using an extended trapezoidal Rule (ETR) with $k = 3$ as described in [17]. We expect this method to be unstable due to the eigenvalues in the right half of the complex plane, which is also observed in Fig. 3. In contrast with the other methods, the generalized midpoint-based method with $\nu = 1$ clearly converges to the exact solution. Tables 2 and 3 at $t = 0.3$ confirm this behaviour in more detail. This can also be seen in Fig. 4, which is even more indicative of the divergence of the FTCS and BTCS solutions, in contrast with the converging BVM solution for an increasing number of time steps N_t. Note, that the computation time for BVM grows faster than for the FTCS and BTCS methods, as expected due to the global nature of the method. However, the FTCS and BTCS solutions make no sense at all for this model. Further, it can be seen from the first two columns in Table 2, that, for $\Delta x = 0.0125$ and decreasing values of the time step Δt (with a factor of 4), the error for this BVM method indeed decreases with a factor of (approximately) 16, confirming its second order accuracy.

4.3. A space-fractional heat equation

Our third numerical example is the (left) space-fractional heat equation of order $\frac{3}{2}$ and can be modelled by the PDE:

$$u_t(x,t) = D^{3/2}u(x,t), \quad (x,t) \in [-L, M] \times [0, T], \tag{26}$$

where the (left) Caputo fractional derivative is defined by:

$$D^{3/2}u(x,t) = \frac{1}{\Gamma(\frac{1}{2})} \int_{-L}^{x} \frac{u_{\xi\xi}(\xi,t)}{\sqrt{x-\xi}}\, d\xi.$$

For more details on fractional derivatives, we refer to [10,13,27]. We take the values $L = 6$, $M = 16$ and $T = 2$. Applying a doubling(in space)-splitting(in time) procedure:

$$u_{tt} = (u_t)_t = [D^{3/2}u]_t = D^{3/2}[u_t] = D^{3/2}[D^{3/2}u] = D^3u = u_{xxx},$$

we can re-formulate PDE (26) to the form of system (23), but now with the initial conditions:

$$\begin{cases} u(x,0) = u_0(x) = \mathrm{e}^{-3(x-2)^2}, \\ v(x,0) = u_t(x,0) = D^{3/2}[u(x,0)] = D^{3/2}[u_0(x)], \end{cases}$$

and, homogeneous Dirichlet boundary conditions, instead of the periodic ones. Note that this doubling-splitting principle could be extended to more general p/q-derivatives. Here, it changes the matrix $\mathcal{D}_3$ in (24) only in the first two and last two rows. One good reason to apply the doubling-splitting to the fractional PDE, is that the fractional derivative (a

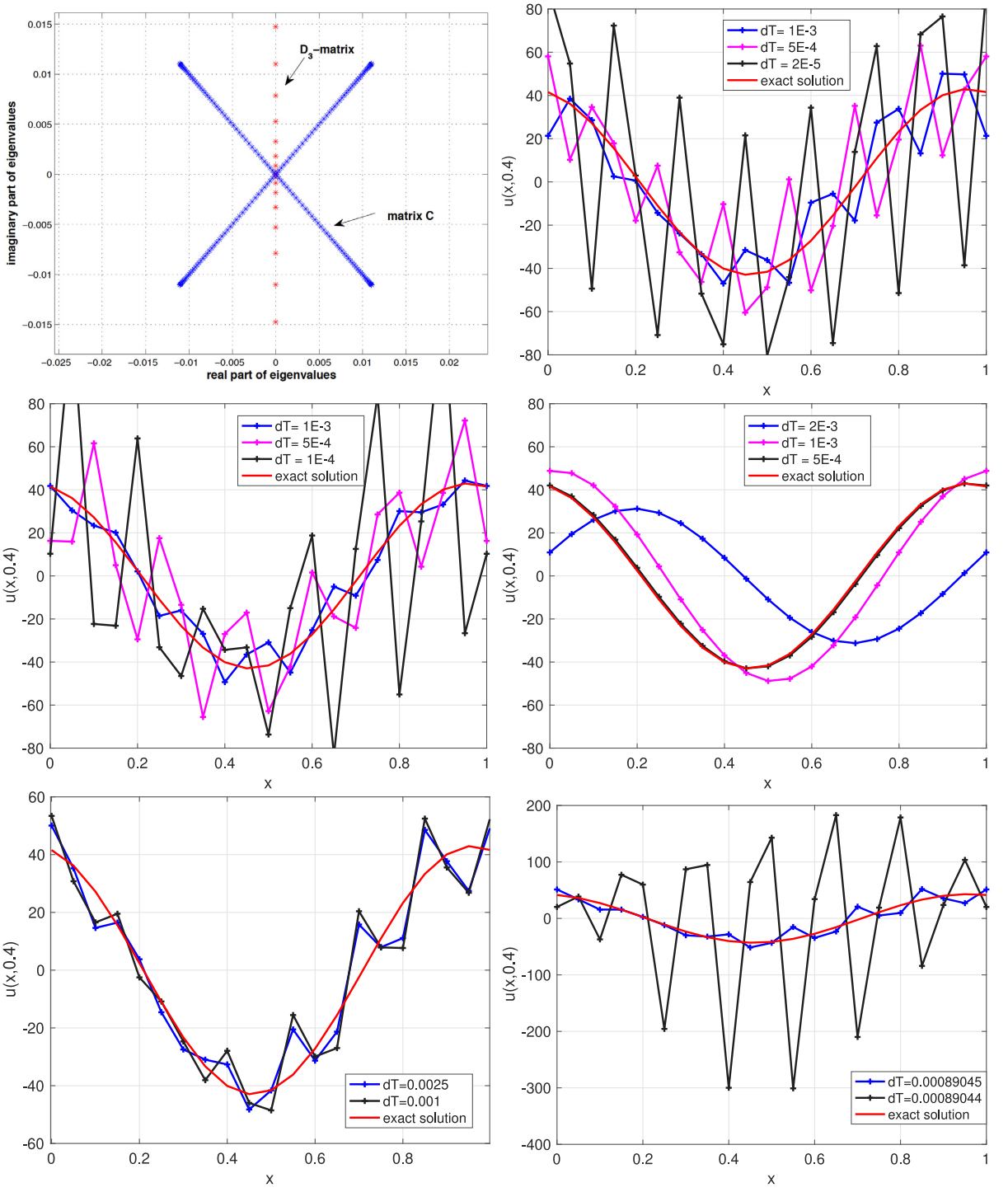

Fig. 3. In the upper left frame, the eigenvalue distributions are shown for the $\mathcal{D}_3$-matrix and the $\mathcal{C}$-matrix in the semi-discrete model (24). The upper right and middle left frames, respectively, show the FTCS and BTCS solutions for decreasing values of the time step Δt. A clear divergence (instability) can be observed. On the other hand, in the middle right frame, the BVM ($\nu = 1$) solution displays a convergent behaviour for decreasing values of the time step Δt. As a comparison, in the two lower frames, numerical solutions are displayed for the ETR(3) BVM-method. Note the irregular behaviour of the solutions for decreasing values of Δt, especially, the sensibility with respect to small changes in Δt in the lower right frame.

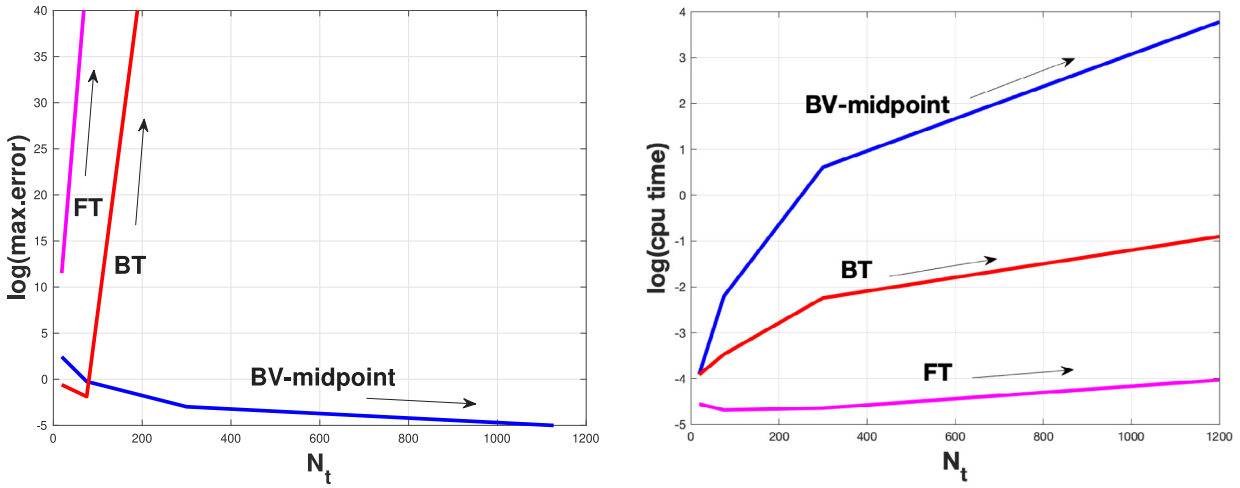

Fig. 4. Left frame: divergence of FTCS and BTCS and convergence of the BVM solutions as a function of the number of time steps N_t for model (22) at $t = 0.4$ with spatial stepsize $\Delta x = 0.01$. Right frame: CPU time for the three methods as a function of N_t.

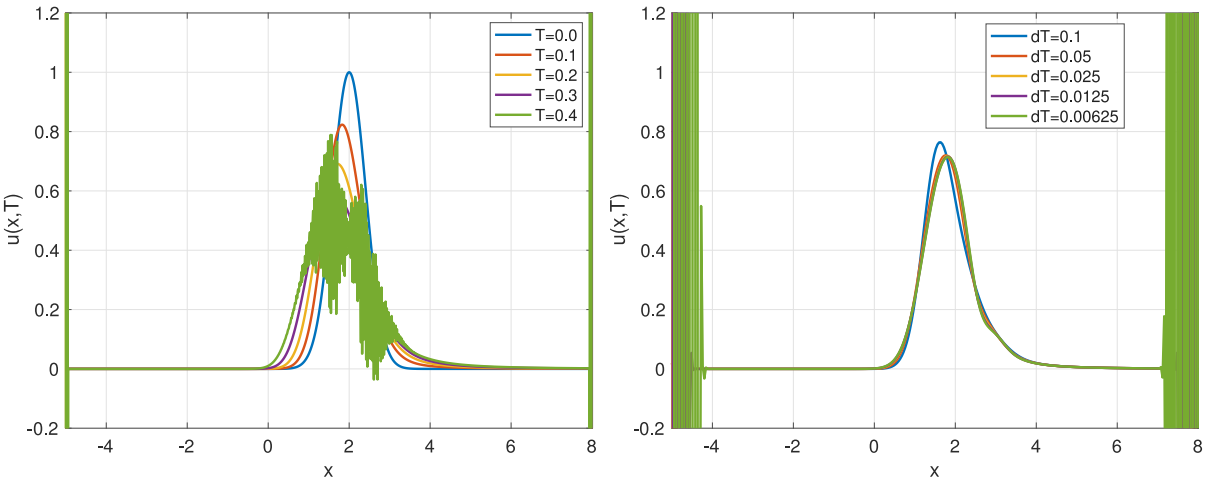

Fig. 5. Unstable solutions with explicit Euler for PDE model (26) after applying the doubling-splitting approach. Left frame: numerical solutions for $t = 0.0, 0.1, \ldots, 0.4$ with $\Delta x = 0.05$ and $\Delta t = 0.01$ (at $t = 0.4$ the numerical solution becomes unstable). Right frame: at $t = 0.1$ decreasing values of Δt yield unstable solutions.

nonlocal operator) only needs to be evaluated at initial time $t = 0$, resulting in a sparse matrix $\mathcal{C}$. In Fig. 5 unstable FTCS solutions (increasing t-values in the left frame, decreasing Δt values in the right frame) and in Fig. 6 similarly for BTCS, the impossibility is illustrated for IVMs to deal with the instabilities caused by the eigenvalue distributions of the semi-discrete system. On the other hand, Fig. 7 nicely shows that the generalized midpoint-based BVM with $\nu = 1$ *is* indeed able to numerically solve this PDE model. For comparison, the lower frame in Fig. 7 displays accurate numerical solutions of the original space-fractional heat Eq. (26). These reference solutions were obtained by applying the numerical discretization as discussed in Ref. [28].

4.4. The backward heat equation in 1D

Our final example is the backward (or inverse) heat equation:

$$\begin{cases} u_t(x,t) = -u_{xx}(x,t), & (x,t) \in [0,1] \times [0,T], \\ u(x,0) = \sin(\pi x), & u(0,t) = u(1,t) = 0, \end{cases} \tag{27}$$

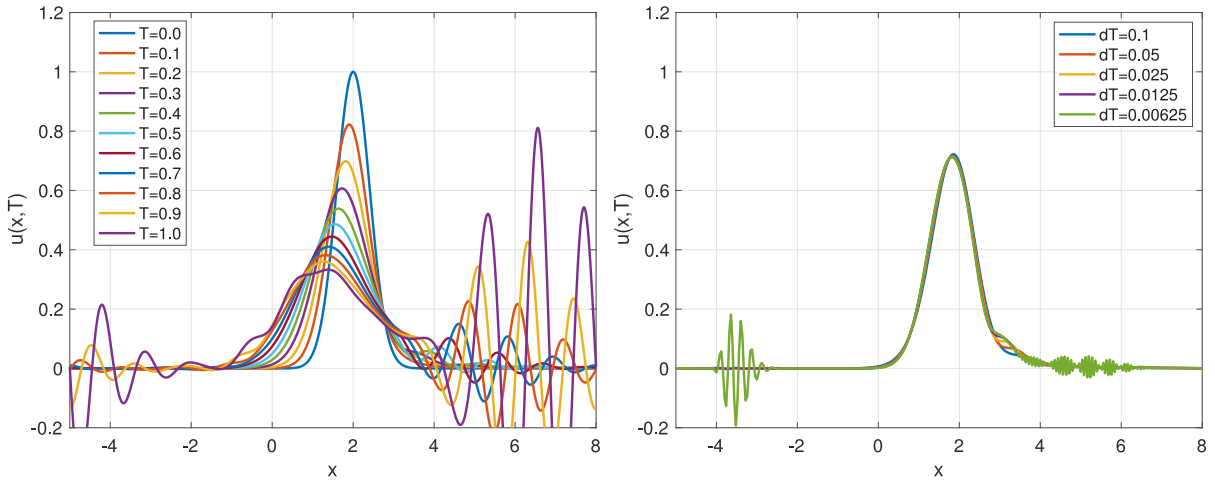

Fig. 6. Unstable numerical solutions with implicit Euler for PDE model (26). Left frame: numerical solutions for $t = 0.0, 0.1, \ldots, 1.0$ with $\Delta x = 0.05$ and $\Delta t = 0.01$ (at around $t = 0.4$ the numerical solution becomes unstable). Right frame shows a similar behaviour: at $t = 0.1$ for decreasing values of Δt.

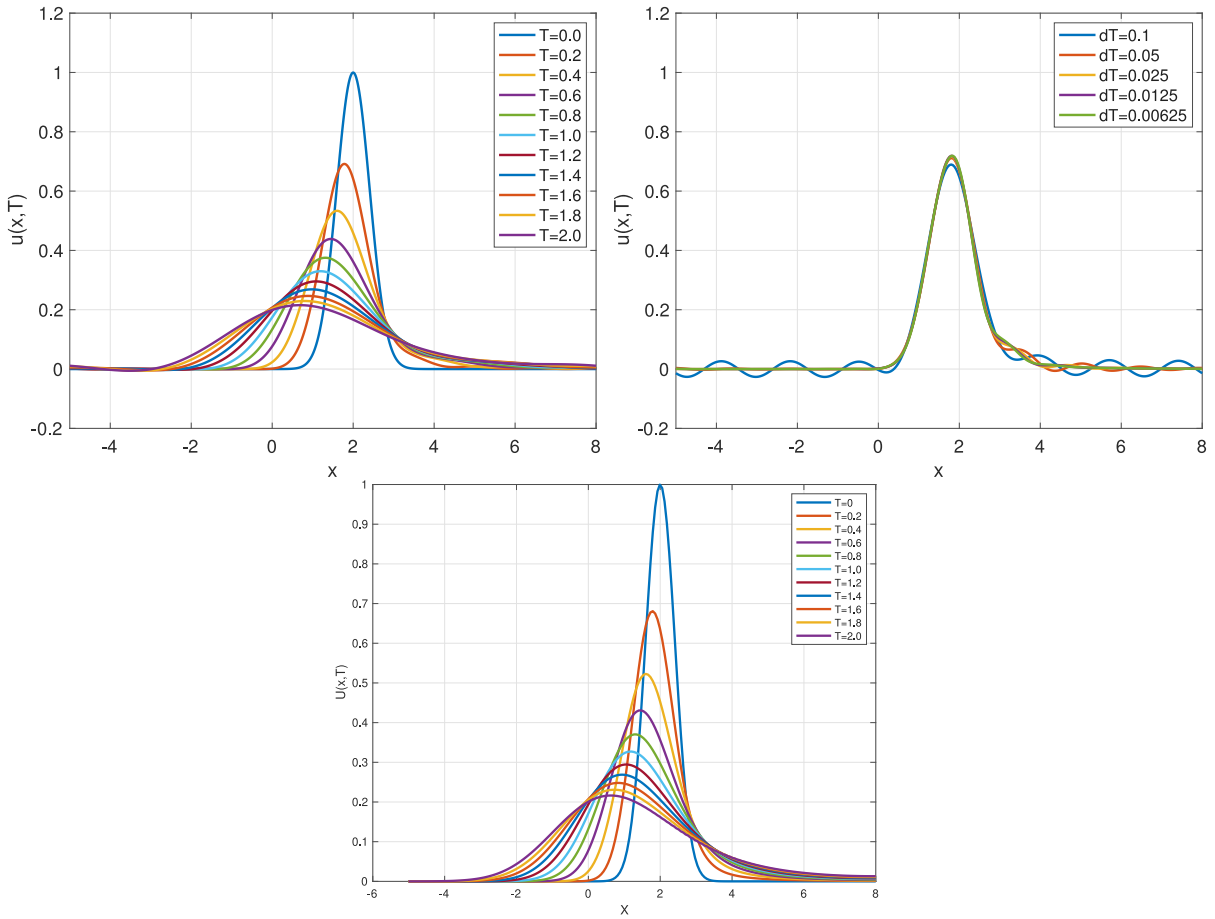

Fig. 7. Stable numerical solutions with BVM ($\nu = 1$) for PDE model (26). Upper left frame: numerical solutions for $t = 0.0, 0.2, \ldots, 2.0$ with $\Delta x = 0.05$ and $\Delta t = 0.01$. Upper right frame: at $t = 0.1$ decreasing values of Δt now yield **stable** solutions. Lower frame: for comparison with the BVM solution, we show accurate numerical solutions of the original space-fractional heat Eq. (26).

Table 4
FTCS solutions for the backward heat model (27): maximum absolute errors and cpu time at $t = 0.25$ for decreasing values of Δx and Δt (the error **explodes**).

FTCS	$\Delta x = 0.1$	*sec*	$\Delta x = 0.05$	*sec*	$\Delta x = 0.025$	*sec*
$\Delta t = 0.025$	2.04	$\mathcal{O}(10^{-3})$	1.96	$\mathcal{O}(10^{-3})$	$\mathcal{O}(10^{3})$	$\mathcal{O}(10^{-4})$
$\Delta t = 0.0125$	1.46	$\mathcal{O}(10^{-3})$	$\mathcal{O}(10^{8})$	$\mathcal{O}(10^{-4})$	$\mathcal{O}(10^{19})$	$\mathcal{O}(10^{-4})$
$\Delta t = 0.00625$	$\mathcal{O}(10^{4})$	$\mathcal{O}(10^{-3})$	$\mathcal{O}(10^{24})$	$\mathcal{O}(10^{-4})$	$\mathcal{O}(10^{46})$	$\mathcal{O}(10^{-4})$
$\Delta t = 0.003125$	$\mathcal{O}(10^{10})$	$\mathcal{O}(10^{-3})$	$\mathcal{O}(10^{44})$	$\mathcal{O}(10^{-4})$	$\mathcal{O}(10^{87})$	$\mathcal{O}(10^{-4})$

Table 5
BTCS solutions for the backward heat model (27): maximum absolute errors and cpu time at $t = 0.25$ for decreasing values of Δx and Δt (again, the error **explodes**).

BTCS	$\Delta x = 0.1$	*sec*	$\Delta x = 0.05$	*sec*	$\Delta x = 0.025$	*sec*
$\Delta t = 0.025$	3.29	$\mathcal{O}(10^{-4})$	3.52	$\mathcal{O}(10^{-3})$	11.74	$\mathcal{O}(10^{-3})$
$\Delta t = 0.0125$	$\mathcal{O}(10^{12})$	$\mathcal{O}(10^{-3})$	$\mathcal{O}(10^{3})$	$\mathcal{O}(10^{-3})$	628.4	$\mathcal{O}(10^{-3})$
$\Delta t = 0.00625$	$\mathcal{O}(10^{17})$	$\mathcal{O}(10^{-3})$	$\mathcal{O}(10^{36})$	$\mathcal{O}(10^{-3})$	$\mathcal{O}(10^{49})$	$\mathcal{O}(10^{-3})$
$\Delta t = 0.003125$	$\mathcal{O}(10^{150})$	$\mathcal{O}(10^{-3})$	$\mathcal{O}(10^{103})$	$\mathcal{O}(10^{-3})$	$\mathcal{O}(10^{65})$	$\mathcal{O}(10^{-3})$

Table 6
BVM solutions ($\nu = 1$) for the backward heat model (27): maximum absolute errors and cpu time at $t = 0.25$ for decreasing values of Δx and Δt. We observe numerical convergence (and the solutions remain stable). It is obvious that the cpu time for BVM grows rapidly for smaller values of Δt and Δx.

BVM ($\nu = 1$)	$\Delta x = 0.1$	*sec*	$\Delta x = 0.05$	*sec*	$\Delta x = 0.025$	*sec*
$\Delta t = 0.025$	73.3	0.023	58.4	0.009	55.7	0.017
$\Delta t = 0.0125$	6.14	0.016	6.83	0.021	7.01	0.038
$\Delta t = 0.00625$	1.12	0.030	1.37	0.054	1.43	0.095
$\Delta t = 0.003125$	0.11	0.087	0.30	0.157	0.35	0.322

with exact solution $u(x, t) = \mathrm{e}^{\pi^2 t} \sin(\pi x)$. We approximate the spatial derivative with the second-order central difference:

$$u_{xx}|_{x=x_i} \approx \frac{1}{(\Delta x)^2}\Big(u_{i+1} - 2u_i + u_{i-1}\Big).$$

The matrix corresponding to the resulting system of ODEs has strictly positive real eigenvalues. Thus, this problem cannot be solved safely using an IVM as can be seen from Tables 4 and 5, where $T = 0.25$. In Table 4 we see that the errors when applying FTCS increase as Δt and Δx decrease. In Table 5 we see a similar behaviour of the error for BTCS, but only once Δx and Δt become sufficiently small. On the other hand, in Table 6 we see that the errors when using the first generalized midpoint-based BVM decrease as Δt tends to zero, but slightly increase as Δx tends to zero. Again, it can be observed in this Table, that, for a fixed value of Δx and halving the time step Δt, the error (approximately) goes down with a factor of 4, which reflects the second-order accuracy, even for this unstable PDE model.

The behaviour of these errors as Δt tends to zero is easily explained by considering the stability regions of the applied methods. To understand the behaviour of the errors as Δx tends to zero we have to consider the eigenvalues of the linear system of ODEs that results from the spatial discretization. As Δx decreases, the maximum of these eigenvalues increases, so the system of ODEs becomes progressively more unstable as Δx decreases.

In Fig. 8, the behaviour of the relative error is shown for the first seven generalized midpoint-based BVMs with fixed Δx, varying values of Δt and $T = 1$. As expected, for increasing ν, the error decreases due to the increased order of accuracy of the method. On the other hand, for $\nu = 7$ we see that the errors start to increase again. This is likely due to the ill-conditioning of the linear system that results from applying the BVM. We hypothesize that this ill-conditioning is due to either the choice of boundary conditions or due to the increasing ratio between the α-coefficients of the generalized midpoint LMF as ν increases.

Lastly, Fig. 9 shows the computation times of the computations that were performed to obtain Fig. 8. As expected, the computation time increases as Δt decreases. Moreover, the computation time increases as ν increases. This is also expected as an increase in ν leads to a reduced sparsity of the resulting system of linear equations that has to be solved.

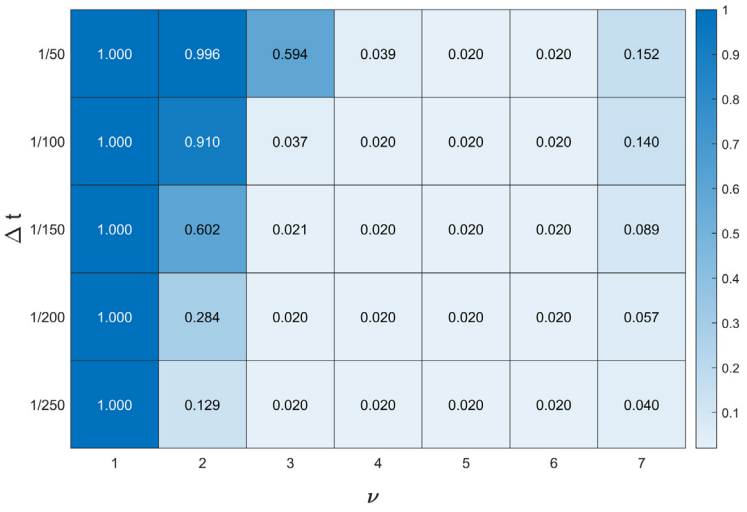

Fig. 8. For the inverse heat Eq. (27) with $\Delta x = 0.05$, we display here the effect of varying the parameter ν in the generalized midpoint-based BVM method (6), (8), (9). On the horizontal axis the ν-value is increased from 1 to 7, whereas the vertical axis in the table displays the variation in Δt from 0.02, 0.01, …, 0.004. The relative error at $t = 1$ is indicated by the blue colour: the darker the colour, the greater the error. We observe for higher values of ν an expected decrease of the relative error, but for $\nu \geq 5$ the error starts increasing again. This is likely due to ill-conditioning of the BVM-matrix for these values. We hypothesize that this ill-conditioning is either due to the choice of boundary conditions or due to the increasing ratio between the α-coefficients of the generalized midpoint LMF as ν increases.

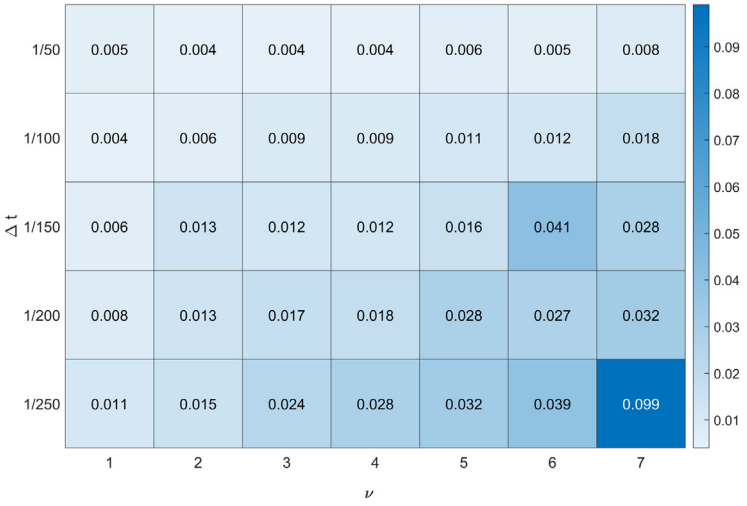

Fig. 9. Computation times of the computations performed to obtain Fig. 8. Note the increase in computation time as ν increases, which results from a decrease of sparsity of the linear system that is obtained by applying the BVM.

5. Conclusion

In this paper we have introduced the class of generalized midpoint-based BVMs. This class of integration methods for solving systems of ODEs has the favourable property of being unconditionally stable. As was shown in the numerical examples, this property makes these methods an attractive option when dealing with (semi-)stable differential equations. However, this unconditional stability comes at the cost of a significant increase in both time and space complexity. Apart from the theoretical discussion that will be given in the future paper [25], many other points of interest remain, such as:

- Optimization of the methods used for solving the linear systems that result from applying a BVM;
- Application of the generalized midpoint-based BVMs to nonlinear partial differential equations;

- Theoretical and numerical investigation into the effects of the choice of boundary conditions on the conditioning of the resulting system of equations;
- Investigation into the correct application of BVMs in combination with the method of lines when applied to PDEs.

Data availability

No data was used for the research described in the article.

Acknowledgements

We would like to thank the anonymous reviewers for their valuable comments to improve the article.

Funding

This research did not receive any specific grant from funding agencies in the public, commercial, or not-for-profit sectors.

Appendix A. Validity of boundary conditions

First, note that the final conditions are trivially of the order k as the coefficients satisfy Eq. (10) and, therefore, the order Eq. (11) up to $s = k$. To prove that the additional initial conditions are also of the order k, it follows from the order Eq. (11) and $\tilde{\alpha}_{j,r} = -\alpha_{j,r}$, that we have to show that

$$\begin{pmatrix} 1 & 1 & \cdots & 1 \\ 0 & 1 & \cdots & k \\ 0 & 1^2 & \cdots & k^2 \\ \vdots & \vdots & & \vdots \\ 0 & 1^k & \cdots & k^k \end{pmatrix} \begin{pmatrix} \alpha_{k,r} \\ \alpha_{k-1,r} \\ \vdots \\ \alpha_{0,r} \end{pmatrix} = - \begin{pmatrix} 0 \\ 1 \\ 2(\nu - r) \\ \vdots \\ k(\nu - r)^{k-1} \end{pmatrix}, \quad r = 1, \ldots, \nu. \tag{A.1}$$

This is equivalent to showing that

$$\sum_{i=0}^{k} i^s \alpha_{k-i,r} = -s(\nu - r)^{s-1}, \tag{A.2}$$

for all $s = 0, \ldots, k$. Now, using Eq. (10) and the binomial theorem, we can write

$$\begin{aligned} \sum_{i=0}^{k} i^s \alpha_{k-i,r} &= \sum_{i=0}^{k} (k-i)^s \alpha_{i,r} \\ &= \sum_{i=0}^{k} \sum_{j=0}^{s} \binom{s}{j} (-1)^{s-j} k^j i^{s-j} \alpha_{i,r} \\ &= \sum_{j=0}^{s} \binom{s}{j} (-1)^{s-j} k^j \sum_{i=0}^{k} i^{s-j} \alpha_{i,r} \\ &= \sum_{j=0}^{s-1} \binom{s}{j} (-1)^{s-j} (2\nu)^j (s-j)(\nu + r)^{s-j-1} \\ &= -s \sum_{j=0}^{s-1} \binom{s-1}{j} (-1)^{s-j-1} (2\nu)^j (\nu + r)^{s-j-1} \\ &= -s(\nu - r)^{s-1}, \end{aligned}$$

where we have used that

$$\begin{aligned}\binom{s}{j}(s-j) &= \frac{s!}{j!(s-j)!}(s-j)\\ &= s\frac{(s-1)!}{j!(s-j-1)!}\\ &= s\binom{s-1}{j}.\end{aligned}$$

Thus, Eq. (A.2) holds, which shows that the coefficients indeed lead to order k approximations.

Appendix B. Midpoint LMF extended coefficient table

k	ν	$\alpha_{\nu-7}$	$\alpha_{\nu-6}$	$\alpha_{\nu-5}$	$\alpha_{\nu-4}$	$\alpha_{\nu-3}$	$\alpha_{\nu-2}$	$\alpha_{\nu-1}$	α_{ν}	$\alpha_{\nu+1}$	$\alpha_{\nu+2}$	$\alpha_{\nu+3}$	$\alpha_{\nu+4}$	$\alpha_{\nu+5}$	$\alpha_{\nu+6}$	$\alpha_{\nu+7}$
10	5			$-\frac{1}{1260}$	$\frac{5}{504}$	$-\frac{5}{84}$	$\frac{5}{21}$	$-\frac{5}{6}$	0	$\frac{5}{6}$	$-\frac{5}{21}$	$\frac{5}{84}$	$-\frac{5}{504}$	$\frac{1}{1260}$		
12	6		$\frac{1}{5544}$	$-\frac{1}{385}$	$\frac{1}{56}$	$-\frac{5}{63}$	$\frac{15}{56}$	$-\frac{6}{7}$	0	$\frac{6}{7}$	$-\frac{15}{56}$	$\frac{5}{63}$	$-\frac{1}{56}$	$\frac{1}{385}$	$-\frac{1}{5544}$	
14	7	$-\frac{1}{24024}$	$\frac{7}{10296}$	$-\frac{7}{1320}$	$\frac{7}{264}$	$-\frac{7}{72}$	$\frac{7}{24}$	$-\frac{7}{8}$	0	$\frac{7}{8}$	$-\frac{7}{24}$	$\frac{7}{72}$	$-\frac{7}{264}$	$\frac{7}{1320}$	$-\frac{7}{10296}$	$\frac{1}{24024}$

Appendix C. Boundary condition coefficient table

k	ν	r	$\alpha_{0,r}$	$\alpha_{1,r}$	$\alpha_{2,r}$	$\alpha_{3,r}$	$\alpha_{4,r}$	$\alpha_{5,r}$	$\alpha_{6,r}$	$\alpha_{7,r}$	$\alpha_{8,r}$
2	1	1	$\frac{1}{2}$	-2	$\frac{3}{2}$						
4	2	1	$-\frac{1}{12}$	$\frac{1}{2}$	$-\frac{3}{2}$	$\frac{5}{6}$	$\frac{1}{4}$				
4	2	2	$\frac{1}{4}$	$-\frac{4}{3}$	3	-4	$\frac{25}{12}$				
6	3	1	$\frac{1}{60}$	$-\frac{2}{15}$	$\frac{1}{2}$	$-\frac{4}{3}$	$\frac{7}{12}$	$\frac{2}{5}$	$-\frac{1}{30}$		
6	3	2	$-\frac{1}{30}$	$\frac{1}{4}$	$-\frac{5}{6}$	$\frac{5}{3}$	$-\frac{5}{2}$	$\frac{77}{60}$	$\frac{1}{6}$		
6	3	3	$\frac{1}{6}$	$-\frac{6}{5}$	$\frac{15}{4}$	$-\frac{20}{3}$	$\frac{15}{2}$	-6	$\frac{49}{20}$		
8	4	1	$-\frac{1}{280}$	$\frac{1}{28}$	$-\frac{1}{6}$	$\frac{1}{2}$	$-\frac{5}{4}$	$\frac{9}{20}$	$\frac{1}{2}$	$-\frac{1}{14}$	$\frac{1}{168}$
8	4	2	$\frac{1}{168}$	$-\frac{2}{35}$	$\frac{1}{4}$	$-\frac{2}{3}$	$\frac{5}{4}$	-2	$\frac{19}{20}$	$\frac{2}{7}$	$-\frac{1}{56}$
8	4	3	$-\frac{1}{56}$	$\frac{1}{6}$	$-\frac{7}{10}$	$\frac{7}{4}$	$-\frac{35}{12}$	$\frac{7}{2}$	$-\frac{7}{2}$	$\frac{223}{140}$	$\frac{1}{8}$
8	4	4	$\frac{1}{8}$	$-\frac{8}{7}$	$\frac{14}{3}$	$-\frac{56}{5}$	$\frac{35}{2}$	$-\frac{56}{3}$	14	-8	$\frac{761}{280}$

Appendix D. Absolute stability of BVMs

We restrict ourselves to the case of the linear test equation, we consider Δt to be fixed and we assume the absence of rounding errors. Suppose we have some IVM with a non-empty region of absolute stability and suppose $q = \lambda\Delta t$ is contained within this region. Then, as the name suggests, the IVM is considered to be absolutely stable. This property is actually based on the system of finite difference equations (FDEs) that results from applying this IVM together with the fixed Δt. This system is of the form

$$u_{n+k} = f(n, u_n, u_{n+1}, \ldots, u_{n+k-1}), \quad 0 \le n \le N-k, u_0 = c_0, \ldots, u_{k-1} = c_{k-1}, \tag{D.1}$$

where the c_i's are the boundary conditions. There are two properties that this system of FDEs should have. Namely, (asymptotic) stability with respect to perturbations of their boundary conditions and uniform stability with respect to global perturbations. These are given in [17] as:

Definition D.1. The solution $\{u_n\}_{n=0}^{N}$ to a system of FDEs of the form (D.1) is, *with respect to perturbations of the boundary conditions*,

- *stable* if, for any $\epsilon > 0$, there exists $\delta > 0$ such that, if the perturbations of the boundary conditions are bounded by δ, then the distance between the perturbed and unperturbed solutions is bounded by ϵ;

- *asymptotically stable* if, for any $\epsilon > 0$, there exists $\gamma > 0$ such that, if the perturbations of the boundary conditions are bounded by γ, the distance between the perturbed and unperturbed solutions tends to zero as n and N tend to infinity.

Definition D.2. The solution $\{u_n\}_{n=0}^{N}$ to a system of FDEs of the form (D.1) is, *with respect to global perturbations*,

- *stable* if, for any $\epsilon > 0$, there exists $\delta > 0$ such that, if the global perturbations are bounded by δ, the distance between the perturbed and the unperturbed solutions is bounded by ϵ.
- *uniformly stable* if, for the solution is stable and δ can be chosen independent of N.

It can be shown, as is done in [17], that the solution to a system of FDEs is stable both with respect to perturbations of the boundary conditions and with respect to global perturbations if the corresponding characteristic polynomial is Von Neumann. When the characteristic polynomial is Schur, one obtains the stronger properties of asymptotic stability with respect to boundary conditions and uniform stability with respect to global perturbations. These stronger types of stability are preferable, which is why the definition of the region of absolute stability uses Schur polynomials.

These definitions can be extended to the case of BVMs. The major difference lies in the type of system of FDEs that results from applying a BVM, as this is now a system with initial and final conditions instead of merely initial conditions. So the system is of the form

$$\begin{aligned} u_{n+k} &= f(n, u_n, u_{n+1}, \ldots, u_{n+k-1}), \quad 0 \le n \le N-k, \\ u_0 = c_0, \ldots, u_{k_1-1} &= c_{k_1-1}, u_{N-k_2+1} = c_{N-k_2+1}, \ldots, u_N = c_N. \end{aligned} \tag{D.2}$$

Note that we do not need to change the definitions of stability with respect to global perturbations. However, for stability with respect to perturbations of the boundary conditions, a small change is necessary. For such a system we propose the following generalized definition

Definition D.3. The solution $\{u_n\}_{n=0}^{N}$ to a system of FDEs of the form (D.2) is, *with respect to perturbations of the boundary conditions*,

- *stable* if, for any $\epsilon > 0$, there exists $\delta > 0$ such that, if the perturbations of the boundary conditions are bounded by δ, then the distance between the perturbed and unperturbed solutions is bounded by ϵ;
- *asymptotically stable* if, for any $\epsilon > 0$, there exists $\gamma > 0$ such that, if the perturbations of the boundary conditions are bounded by γ, the distance between the perturbed and unperturbed solutions tends to zero as N and $\min(n, N-n)$ tend to infinity.

Now, for a system of FDEs of the form (D.2), we can show that its solution is uniformly stable with respect to perturbations of its boundary conditions and asymptotically stable with respect to global perturbations when its characteristic polynomial is $S_{k_1 k_2}$. The proof of this result is fairly long and will therefore be given in detail in another paper. Here we will provide a sketch of this proof, which is a generalization of the aforementioned proof in [17] and which uses similar techniques.

We will first consider the asymptotic stability with respect to perturbations of the boundary conditions. First, let $z_1, \ldots, z_k$ denote that roots of the characteristic polynomial of the system of FDEs, ordered such that $|z_i| \le |z_j|$. Then, define the mosaic Vandermonde matrix

$$W^{(k_1,k_2)} = \begin{pmatrix} 1 & \cdots & 1 & 1 & \cdots & 1 \\ z_1 & \cdots & z_{k_1} & z_{k_1+1} & \cdots & z_k \\ \vdots & & \vdots & \vdots & & \vdots \\ z_1^{k_1-1} & \cdots & z_{k_1}^{k_1-1} & z_{k_1+1}^{k_1-1} & \cdots & z_k^{k_1-1} \\ z_1^{N} & \cdots & z_{k_1}^{N} & z_{k_1+1}^{N} & \cdots & z_k^{N} \\ \vdots & & \vdots & \vdots & & \vdots \\ z_1^{N+k_2-1} & \cdots & z_{k_1}^{N+k_2-1} & z_{k_1+1}^{N+k_2-1} & \cdots & z_k^{N+k_2-1} \end{pmatrix},$$

the diagonal matrix

$$D = \operatorname{diag}(z_1, \ldots, z_k)$$

and the vector

$$E = (1, \ldots, 1)^T \in \mathbb{R}^k.$$

Then, Brugnano and Trigiante have shown in [17] that we can write the distance between the perturbed and unperturbed solutions as

$$e_n = E^T D^n (W^{(k_1,k_2)})^{-1} \begin{pmatrix} e_0 \\ \vdots \\ e_{k_1-1} \\ e_{N-k_2+1} \\ \vdots \\ e_N \end{pmatrix},$$

where $e_0, \ldots, e_{k_1-1}, e_{N-k_2+1}, \ldots, e_N$ are the perturbations of the boundary conditions. By using a block LU decomposition of the matrix $W^{(k_1,k_2)}$ and the fact that the corresponding characteristic polynomial is $S_{k_1k_2}$, the term $D^n(W^{(k_1,k_2)})^{-1}$ can be rewritten to a form from which it is obvious that the term tends to the zero matrix as N and $\min(n, N-n)$ tend to infinity. Therefore, the solution of the system of FDEs is asymptotically stable with respect to perturbations of the boundary conditions.

For showing uniform stability with respect to global perturbations, we first write the differences between the perturbed and unperturbed equations $\vec{e} = (e_{k_1}, \ldots, e_{N-k_2})$ as

$$T_N \vec{e} = \vec{\tau},$$

where we use the Toeplitz matrix

$$T_N = \begin{pmatrix} p_{k_1} & \cdots & p_k & & & \\ \vdots & \ddots & & \ddots & & \\ p_0 & & \ddots & & \ddots & \\ & \ddots & & \ddots & & p_k \\ & & \ddots & & \ddots & \vdots \\ & & & p_0 & \cdots & p_{k_1} \end{pmatrix},$$

where the p_i are the coefficients of the BVM and where we use the vector of perturbations $\vec{\tau} = (\tau_{k_1}, \ldots, \tau_{N-k_2})^T$. Brugnano and Trigiante have used the fact that the characteristic polynomial defined by the p_i being $S_{k_1k_2}$ leads to

$$|T_N^{-1}| \leq \alpha\,(I_N + \Delta_N + \Delta_N^T),$$

for some $\alpha > 0$ and $0 < \gamma < 1$, which are independent of N and where

$$\Delta_N = \begin{pmatrix} 0 & \gamma & \cdots & \gamma^{N-1} \\ 0 & 0 & \ddots & \vdots \\ \vdots & & \ddots & \gamma \\ 0 & \cdots & \cdots & 0 \end{pmatrix}.$$

For fixed $\epsilon > 0$, this bound and the fact that $\sum_{i=0}^{\infty} \gamma^i$ is finite can be used to find a proper choice of δ, independent of N, such that the elements of $\vec{e}$ are bounded by ϵ, which shows uniform stability with respect to global perturbations.

Asymptotic stability with respect to perturbations of the boundary conditions and uniform stability with respect to global perturbations together show that the truncation errors, introduced by the additional boundary conditions and by the LMF itself, do not lead to large errors overall if they are sufficiently small. Thus, if Δt is chosen sufficiently small for some convergent (k_1, k_2)-BVM and if the resulting characteristic polynomial is indeed of type $S_{k_1k_2}$, then the solution will be stable.

References

[1] A. Kapila, Asymptotic Treatment of Chemically Reacting Systems, Pitman Advanced Publishing Program, 1983.
[2] J.D. Buckmaster, The mathematics of combustion, Soc. Ind. Appl. Math. (1985).
[3] L. Martinez Alonso, A.B. Shabat, Towards a theory of differential constraints of a hydrodynamic hierarchy, J. Nonlinear Math. Phys. 10 (2003) 229–242.

[4] Y.P. Apakov, S. Rutkauskas, On a boundary value problem to third order PDE with multiple characteristics, Nonlinear Anal. Model. Control 16 (2011) 255–269.
[5] R. Hernandez-Herdero, A. Shabat, V. Sokolov, A new class of linearizable equations, J. Phys. A (2003).
[6] S.I. Kabanikhin, Invers and Ill-Posed Problems: Theory and Applications, De Gruyter Inc, 2011.
[7] J.V. Beck, B. Blackwell, C.R. St.Clair Jr., Inverse Heat Conduction: Ill-Posed Problems, John Wiley & Sons Inc., 1985.
[8] Z. Han, Y. Huang, M. Jian, Inverse problems for equations of parabolic type, in: Ch.1 in Perspectives in Mathematical Sciences, vol. 9, 2009, pp. 93–113.
[9] Y. Yu, X. Luo, H. Zhang, Q. Zhang, The solution of backward heat conduction problem with piecewise linear heat transfer coefficient, Mathematics 7 (2019) 388.
[10] R. Hilfer, Applications of Fractional Calculus in Physics, World Scientific Publishing Co., 2000.
[11] A.A. Kilbas, H.M. Srivastava, J.J. Trujillo, Theory and Applications of Fractional Differential Equations, in: North-Holland, Mathematics Studies, vol. 204, 2006.
[12] B. Ross, Fractional Calculus and Applications, in: Lecture Notes in Mathematics, vol. 457, Springer-Verlag, NewYork-Berlin, 1974.
[13] R. Hermann, Fractional Calculus: An Introduction for Physicists, World Scientific Publishing Co., 2014.
[14] E. Hairer, S.P. Nørsett, G. Wanner, Solving Ordinary Differential Equations I: Nonstiff Problems, second revised ed., Springer-Verlag, Berlin, Heidelberg, 2008.
[15] E. Hairer, G. Wanner, Solving Ordinary Differential Equations II: Stiff and Differential-Algebraic Problems, Springer-Verlag, Berlin, Heidelberg, 1991.
[16] W. Hundsdorfer, J.G. Verwer, Numerical Solution of Time-Dependent Advection-Diffusion-Reaction Equations, Springer-Verlag, Berlin, Heidelberg, 2003.
[17] L. Brugnano, D. Trigiante, Solving Differential Problems by Multistep Initial and Boundary Value Methods, Gordon and Breach, Amsterdam, 1998.
[18] L. Aceto, D. Trigiante, The stability problem for linear multistep methods: Old and new results, J. Comput. Appl. Math. 210 (1–2) (2007) 2–12.
[19] L. Aceto, C. Magherini, On the relations between B2VMs and Runge–Kutta collocation methods, J. Comput. Appl. Math. 231 (1) (2009) 11–23.
[20] A.O.H. Axelsson, J.G. Verwer, Boundary value techniques for initial value problems in ordinary differential equations, Math. Comp. 45 (1985) 153–171.
[21] L. Brugnano, D. Trigiante, Convergence and stability of boundary value methods for ordinary differential equations, J. Comput. Appl. Math. 66 (1996) 97–109.
[22] J.C. Butcher, Numerical Methods for Ordinary Differential Equations, second ed., John Wiley & Sons, West Sussex, 2008.
[23] P. Amodio, F. Mazzia, A boundary value approach to the numerical solution of initial value problems by multistep methods, J. Difference Equ. Appl. 1 (1995) 353–367.
[24] P. Ghelardoni, P. Marzulli, Stability of some boundary value methods for IVPs, Appl. Numer. Math. 18 (1995) 141–153.
[25] M.W.F. van Spengler, P.A. Zegeling, Unconditional stability of generalized midpoint-based boundary value methods with a fixed time step, 2023, in preparation.
[26] MATLAB, Version 9.7.0 (R2019b), The MathWorks inc., Natick, Massachusetts, 2019.
[27] P.A. Zegeling, I. Ateş, A homotopy perturbation method for fractional-order convection-diffusion-reaction boundary-value problems, Appl. Math. Model. 47 (2017) 425–441.
[28] S. Shen, F. Liu, Error analysis of an explicit finite difference approximation for the space fractional diffusion equation with insulated ends, ANZIAM J. V46 (2005) 871–887.